A NEW NMR T_1 MEASUREMENT TECHNIQUE FOR GAS SHALE, HEAVY OIL, AND MICROPOROSITY CHARACTERIZATIONS

Songhua Chen and Lilong Li
Halliburton Energy Services, Houston, Texas, USA

This paper was prepared for presentation at the International Symposium of the Society of Core Analysts held in Aberdeen, Scotland, UK, 27-30 August, 2012

ABSTRACT

This paper describes a new approach of using a hybrid saturation-inversion-recovery (HSIR) sequence for T_1 measurements. The magnetization evolution of the HSIR sequence is described, and extensive simulations are reported for the comparison of the T_1 distributions derived from HSIR and saturation recovery (SR) sequence. Because HSIR and SR require different data acquisition time, we designed our comparison test based on a total fixed-acquisition-time scenario. This equal-time scenario is equivalent to the equal-logging speed condition; thus, the outcome is directly applicable for NMR logging operation. Random noise is added such that the targeted SNR of the time-domain magnetization evolutions from these two sequences are representative to laboratory core measurements and logging measurements, respectively. To test the fidelity of the T_1 distribution results derived from inversion with the true T_1 distribution, Fréchet distances are computed and compared. It is found that the Fréchet distance is shorter for T_1 distributions derived from the HSIR sequence than those derived from the SR sequence, thereby providing quantifiable evidence of the advantage of using HSIR over SR for T_1 data acquisition. Furthermore, we determined the optimal acquisition sequence parameter in HSIR sequence using the criteria of minimizing both the Fréchet distance and the curve misfit between the model and inversion results.

INTRODUCTION

Nuclear magnetic resonance (NMR) longitudinal relaxation-time, T_1, distribution is a commonly-used measurement for both core analysis and well logging. It is a preferred technique for LWD NMR [1] because it is less vulnerable to vibration compared to CPMG [2] T_2 measurements. For wireline NMR logging, T_1 data is easier than T_2 to interpret because it is not affected by the additional NMR magnetization decay caused by the molecular diffusion in the presence of magnetic field gradients. Moreover, the ratio of T_1/T_2 depends on fluid and formation characteristics, which is additional information to T_2 measurement alone. Despite these benefits, the commonly-used T_1 data-acquisition methods have their drawbacks. The inversion-recovery (IR) sequence [3], which is often used as the standard laboratory T_1 measurement technique, requires a very long measurement time, thus is not suited for logging operation. On the other hand, the more

logging-friendly saturation-recovery (SR) [3] sequence has the lowest signal strength at short wait times (TW), resulting in a reduced sensitivity in the short relaxation time range. Therefore, there is an increased interest of developing more efficiency T_1 measurements that also have adequate sensitivity for fast relaxing components common to organic shales, heavy oil reservoirs, and microporosity in carbonates.

In this paper, we describe a new approach of using a hybrid saturation-inversion-recovery (HSIR) sequence, which takes advantage of the higher sensitivity for the short inversion times in the IR sequence and the efficient data acquisition feature in the SR sequence. The paper begins with the description of the NMR magnetization evolution, a.k.a. the signal decay function of the HSIR sequence. To demonstrate the benefit of using such a hybrid approach, we simulated many different cases representative to organic-rich shale, heavy oil, and carbonate rocks having various amounts of rapid relaxing components, as well as slow-relaxing components, using the standard SR and new HSIR methods. In core NMR and logging measurements, the time required to obtain the adequate accuracy of the relaxation time-distribution results are important. In the case of logging, the required time directly affects the logging speed in wireline operation, or rate of penetration (ROP) in LWD. Thus, a fair and meaningful comparison of the performance of the two sequences must take into consideration the total data-acquisition time requirement. The equal-acquisition-time condition is equivalent to the equal logging speed or equal ROP condition.

For practical applications, one must compare the performance of the petrophysical meaningful results. While the total porosity is straightforward to compare, the quantification of the fidelity of the T_1 distribution derived from the inversion of the T_1 evolutions of these sequences is more challenging. To the best of our knowledge, no method has reported on this subject. In this paper, we propose using Fréchet distance [4] to quantify the resemblance between two T_1 distributions. In our study, the Fréchet distance is calculated for the comparison of the true (model) T_1 distribution and the T_1 distribution inverted from the magnetization evolutions from either the HSIR or SR sequence. It is found that the Fréchet distance is shorter for T_1 distributions derived from the HSIR sequence than those derived from the SR sequence.

In the comparison study, we added random noise to the time-domain magnetization evolution data such that the noise reaches the typical levels found in either laboratory NMR core plug measurements or openhole logging data, respectively. We also modeled systems with different underlying T_1/T_2 ratio because the ability to resolve the relaxation time spectrum and quantify the fast relaxing components is T_1/T_2 ratio dependent. In each model, simulation is repeated at least 100 realizations with fresh random noises in the magnetization evolution data; the conclusion is based on the statistical measures of the whole data set. We found that the improvements gained by using the HSIR sequence are observed for both core and log-data noise level but are more significant in the high-level noise data, indicating that the sequence is indeed more beneficial to the logging operation.

DESCRIPTION OF HSIR SEQUENCE

The commonly used-pulse sequences for T_1 measurements are the saturation-recovery sequence and inversion-recovery sequence. The current NMR logging techniques for T_1 measurement exclusively uses the saturation recovery followed by the CPMG method for a good reason. The saturation-recovery-CPMG method is illustrated in Fig. 1(a) and is described symbolically by (sat)-TW-π/2–TE/2-(π–TE/2-echo-TE/2)$_n$, where TW is the wait time, TE is the interecho time, (sat) represents a saturation pulse or pulses, and π and π/2 are RF pulses. The inversion-recovery-CPMG method is illustrated in Fig. 1(b) and is described symbolically by π-TI-π/2–TE/2-(π–TE/2-echo-TE/2)$_n$, where TI is the inversion time.

Compared to the IR sequence, the SR sequence does not require a long time to reach full polarization between the measurements of two TWs. In contrast, the IR sequence requires a very long wait time (>3 times the longest T_1 component) to repolarize the magnetization. Therefore, from the logging speed consideration, the SR approach is favored to IR.

The polarization buildup following the saturation pulse is described by

$$M(TW) = M_0(1 - \exp(-TW/T_1)) \quad (1)$$

for a single T_1 component system. For a system containing a multiple component fluid fractions and/or pore sizes, the buildup can be described by

$$M(TW) = \sum_{i=1}^{N} M_{0i}(1 - \exp(-TW/T_{1i})). \quad (2)$$

It is obvious from Eqs. (1) and (2) that the polarization build-up curve starts from near zero at low *TW*.

On the other hand, using the IR sequence, the polarization evolution is described by

$$M(TI) = M_0\left[1 - 2\exp\left(-\frac{TI}{T_1}\right)\right] \quad (3)$$

for a single T_1 component system, and for a system containing multiple component fluid fractions and/or pore sizes, the buildup can be described by

$$M(TI) = \sum_{i=1}^{N} M_{0i}\left[1 - 2\exp\left(-\frac{TI}{T_{1i}}\right)\right] \quad (4)$$

Obviously, the evolution of magnetization starts at nearly $-M_0$ at very low *TI*.

The commonly-used method to obtain a distribution of T_1 is by inverting the evolution of the magnetization polarization curve with a multiexponential decay model described by

Eq. (2) or (4). Because signals corresponding to different T_{1i} should be greater than or equal to zero, a non-negative constraint is included in the inversion. The sensitivity of inversion to resolve the individual components depends, among others, on the signal-to-noise ratio of the evolution of the polarization curve data. For the saturation-recovery method, the initial data points, corresponding to the short *TW*s, has a very poor SNR; thus, the fast-relaxing components can suffer a greater error. On the other hand, for short *TI*s in the inversion-recovery sequence, the signal amplitude of the initial data points may be close to M_0 but opposite in the phase. Therefore, the SNR may be adequate.

Ideally, one needs a pulse sequence that can overcome the long time required to run the IR sequence but maintain the advantage of this sequence's sensitivity to the fast decay T_1 components. The hybrid sequence described in this paper is an attempt to serve the purpose. The sequence can be described as asaturation-(partial-recovery)-inversion-recovery sequence (HSIR) and can be symbolically written as:

$$(sat) - TW_i - \pi - TI_j - \pi/2 - TE/2 - (\pi - TE/2 - \text{echo} - TE/2)_n.$$

The TW_i can be fixed or variable but is usually a short time interval, which allows only the fastest relaxing component being fully polarized. The first saturation pulse establishes the well-defined state. After TW_i,

$$M(TW_i) = M_0(1 - \exp(-TW_i/T_1)) \tag{5}$$

is the polarized magnitude of the magnetization. The following π pulse inverts this $M(TW_i)$ signal to the –z direction, and the remaining unpolarized magnetization, $M_0 e^{-\frac{TW_i}{T_1}}$, continues its course of building up the polarization. Subsequently, after the inversion-recovery with time TI_j,

$$\mathrm{M} = \mathrm{M}_0 \cdot \left\{ \left(1\text{-}e^{-\frac{\mathrm{TW_i}}{\mathrm{T_1}}}\right) \cdot \left(1\text{-}2e^{-\frac{\mathrm{TI_j}}{\mathrm{T_1}}}\right) + e^{-\frac{\mathrm{TW_i}}{\mathrm{T_1}}} \cdot \left(1\text{-}e^{-\frac{\mathrm{TI_j}}{\mathrm{T_1}}}\right) \right\} \tag{6a}$$

With algebraic simplification, Eq. (6) can be rewritten as:

$$M = M_0 \cdot \left[1 - 2e^{-\frac{TI_j}{T_1}} + e^{-\frac{TI_j + TW_i}{T_1}} \right]. \tag{6b}$$

From this expression, we see that if we choose the TW value sufficient larger than a T_1 component value we want to quantify, the third term in the bracket can be dropped, and we can vary *TI*s to estimate this component. In a latter section, we will show an example of optimization of TW.

Finally, at the end of the CPMG echo train with n number of echoes, the magnetization is described by

$$M = M_0 \cdot \left[1 - 2e^{-\frac{TI_j}{T_1}} + e^{-\frac{TI_j+TW_i}{T_1}}\right] \cdot e^{-\frac{nTE}{(T_1/R)}} \quad (7)$$

for a single relaxation time component system, where we have used $R = T_1/T_2$ instead of explicitly T_2. On the other hand, for a multiple-component system,

$$M(TW_i) = \sum_{k=1}^{K} M_{0k} \cdot \left[1 - 2e^{-\frac{TI_j}{T_{1k}}} + e^{-\frac{TI_j+TW_i}{T_{1k}}}\right] \cdot e^{-\frac{nTE}{(T_{1k}/R_k)}}. \quad (8)$$

Fig. 1 illustrates (a) the SR sequence and (b) the IR sequence, and (c) HSIR sequence; To imitate logging data acquisition, each sequence is followed by a short CPMG echo train.

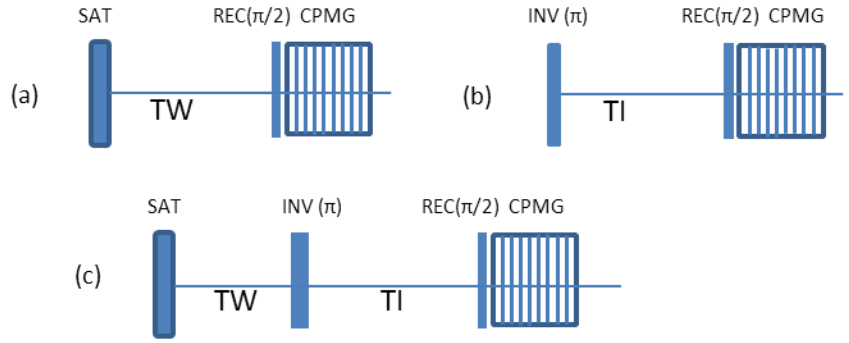

Fig. 1. Illustration of (a) saturation-recovery sequence, (b) inversion recovery sequence, and (c) hybrid saturation-inversion-recovery sequence. Each method is followed by a CPMG echo train acquisition.

SIMULATION MODELS AND PULSE SEQUENCE PARAMETERS

To objectively compare the capability of deriving petrophysical information from the two data acquisition methods, simulation of the magnetization evolutions with response to the same input models are generated with additive random noises at the level comparative to that typically found in (1) core plug NMR measurements and (2) NMR logging data.

The formation rock models are extracted from the observation of real NMR logging data in (1) a North America shale gas well with dominant porosity a in short-relaxation time range, (2) a heavy oil-bearing formation containing heavy oil and movable water, and (3) T_2 distributions of a carbonate reservoir having both micro- and macro-porosities. To add to the complexity of the model, we choose a variable $R = T_1/T_2$ ratio for these models. The R values are set to be 3 for the shortest relaxation time component and 1 for the longest relaxation time component and progressively decrease from 3 to 1 for the

intermediate components. Such a pattern of R variation is reasonable especially for heavy-oil and shale gas formations.

The values of *TW*s and *TI*s in the HSIR sequence are listed in Table 1.

Table 1. The TW and TI times used in the HSIR sequence simulation

TI	0	0.5	1	2	3	4	8	16	40	100	300	500	1000	3000
TW	8	8	8	8	8	0	0	0	0	0	0	0	0	0

The interecho time of these echo trains following the HSIR and SR sequence is 0.3 ms. The number of echoes is 15. With these parameters, the difference in total data-acquisition time between this HSIR and the SR sequences is less than 1%, thus can be considered approximately equal. Note that the TW value is chosen to be zero for TI values greater than 4 ms, because it is no longer necessary for longer TIs and it saves time as well. For the SR sequence, the TW values are chosen the same as the TI values of the HSIP sequence listed in Table 1. Note that we did not include the plain IR sequence in our comparison because it will obviously take very long time so the disadvantage is obvious.

DATA PROCESSING METHODS

The data are inverted in two steps. The first step inverts the echo trains with a multi-T_2 decay model to obtain the apparent porosity vector, $\phi(TW_i, TI_j)$. The second step inverts the $\phi(TW_i, TI_j)$ vector with a multi-T_1 polarization build-up model. The two-step inversion is illustrated in Fig. 2. We choose to use the two-step inversion to eliminate the need for estimating the unknown T_1/T_2 in the inversion process. The inversion processing algorithm included a regularization term where the normal regularization has been used for all data. The regularization coefficient is adjusted based on the signal strength and noise level.

For the quantitative comparison of the T_1 distributions from the inversion with the true T_1 relaxation-time distribution models, the Fréchet distances between the inversion results and the true models are calculated. The Fréchet distance is a measure of similarity between two curves that takes into account the location and ordering of the points along the curves. The shorter the Fréchet distance, the higher degree of similarity between the inversion result and the model T_1 distribution. In our computation, the vertical scale of the partial porosity model is normalized to the same as the horizontal log(T_1) scale. The inversion results are normalized by the same factor. A discrete Fréchet distance computational algorithm, such as that described in Eiter [5], can then be used to compute the distance. To our knowledge, this is the first report of using Fréchet distance as a quantitative measure of the relaxation-time-distribution curve resemblance, and this approach is a reliable measure for not only the model and real inversion data. It can also

be used for comparing core and log-derived relaxation time distributions. As a comparison, we also computed the curve misfit:

$$\sqrt{\sum_{i=1}^{nBins}\left(M_i^{inv}-M_i^{model}\right)^2/\#\ of\ bins}\ . \tag{9}$$

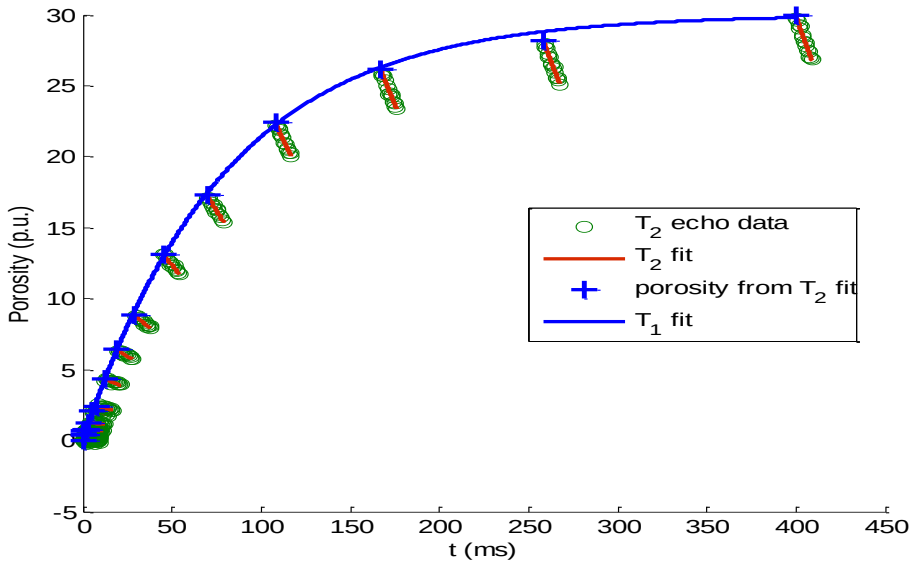

Fig. 2. Illustration of the two-step inversion for an example of the magnetization evolution by SR sequence.

RESULTS

(a) Core-Measurements-Compatible SNR Simulations

Fig. 3 shows the model T_1 distributions representative to (i) carbonate, (ii) heavy oil with movable water, and (iii) black shale formations, as well as multiple noise-realization of the inversion results. The total porosity of these cases are 22 p.u. (carbonate), 15 p.u. (heavy oil reservoir), and 6 p.u. (gas shale), respectively. All cases are simulated with a fixed SNR of 200, in the range for good laboratory core-plug NMR measurements. The left-hand side plots are for the results derived from SR measurements and, the right-hand side plots are for the results derived from the hybrid-pulse sequence.

Using the naked eye, the high SNR data inversion results derived from both SR and HSIR are observed to be quite good. For the heavy-oil and shale cases, the HSIR results recover the model distribution patterns more closely, particularly for the short relaxation-time ranges. This is consistent with our expectation that the HSIR has better sensitivity for the fast-relaxing components.

The Fréchet distances have been computed for all these cases for quantitative comparison between the inversion results derived from these two sequences. The Fréchet distance and the misfit calculation values shown in Table 2 indicated non-trivial improvements for HSIR data vs the SR pulse sequence data. The values listed in the table are the means of the values computed from the individual noise realizations.

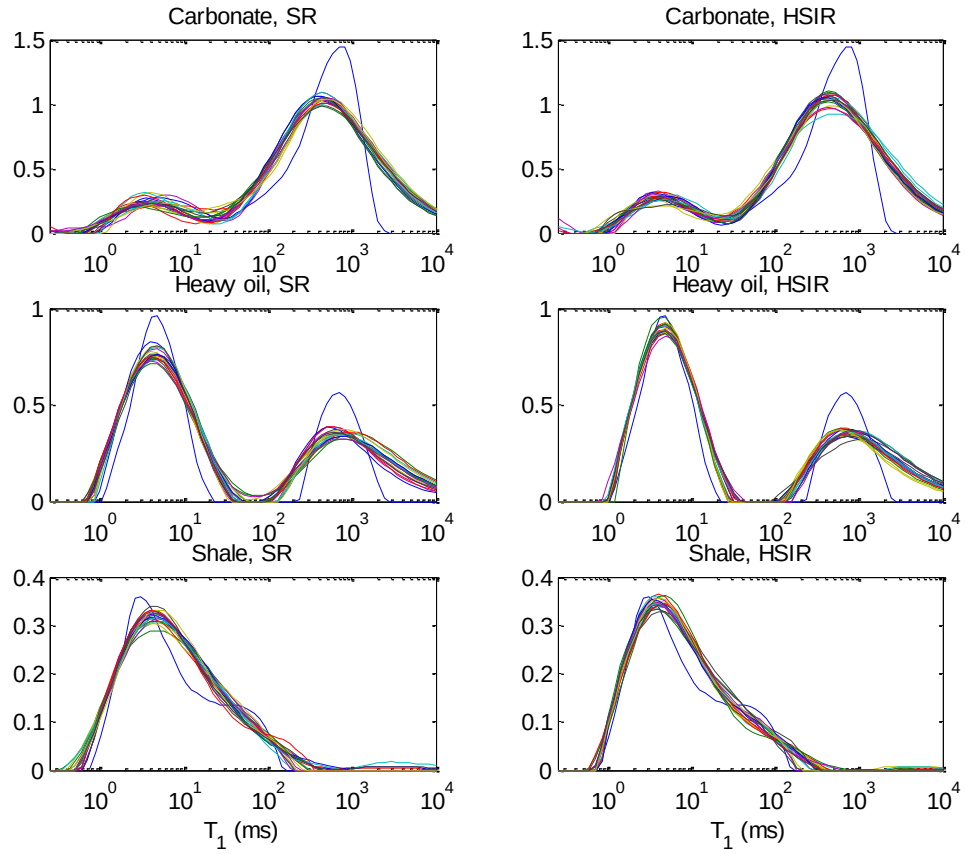

Fig. 3: Comparison between the model (blue curves) and inversion results from SR (left) and HSIR (right) sequences. The SNR is fixed to 200, representative to core-plug measurement quality. The HSIR results recover the model distribution patterns more closely, particularly for the short relaxation-time ranges in the heavy-oil and shale gas cases.

(b) Logging-Data-Compatible SNR Simulations

The more significant improvements are observed when the data have higher levels of noises. In logging operations, the noise level is determined by the formation, borehole environment, tool and acquisition configurations, and the data averaging. In this study, we added 0.5 p.u. of random noise to all the model data. For a 22-, 15-, and 6-p.u. model formations, the corresponding SNR is 44, 30, and 12, respectively, and is in the typical range of logging data quality. The T_1 distribution results are shown in Fig. 4.

Table 2: Statistical analysis of Fréchet Distance and Misfit for the cases shown in Fig. 3

	Mean Fréchet Distance	STD of Fréchet Distance	Mean Misfit	STD of Misfit
Carbonate-SR	2.75	0.23	0.2123	0.0103
Carbonate-HSIR	2.72	0.25	0.2100	0.0107
Heavy Oil-SR	2.22	0.19	0.1285	0.0080
Heavy Oil-HSIR	2.13	0.20	0.1097	0.0080
Shale-SR	1.30	0.19	0.0325	0.0032
Shale-HSIR	1.11	0.01	0.0291	0.0033

Compared to high SNR cases shown in Fig. 3, the improvements by using HSIR sequence are more significant for the low SNR cases (Fig. 4). The quantitative, statistical analysis of the Fréchet distance shows improvement for all cases with more significant improvements achieved for heavy-oil and shale gas cases. The less-significant improvement for carbonates with small amounts of microporosity is understandable because the weak-signal amplitudes at the short relaxation-time range, where the HSIR sequence exhibits the advantage, do not contribute significantly to the Fréchet distance nor to the misfit. Nevertheless, for both the high SNR and low SNR case, HSIR results still consistently show advantage for all cases, and visually, we can see that consistency of the inversion results for HSIR data in the microporosity ranges for varying noise realizations is better than that for the SR data in the same region.

Table 3: Statistical analysis of Fréchet Distance and Misfit for the cases shown in Fig. 4

	Mean Fréchet Distance	STD of Fréchet Distance	Mean Misfit	STD of Misfit
Carbonate-SR	4.07	0.23	0.2545	0.0105
Carbonate-HSIR	4.04	0.23	0.2508	0.0101
Heavy Oil-SR	5.03	0.29	0.2127	0.0105
Heavy Oil-HSIR	3.48	0.24	0.1688	0.0106
Shale-SR	5.20	0.35	0.0705	0.0056
Shale-HSIR	3.76	0.41	0.0513	0.0051

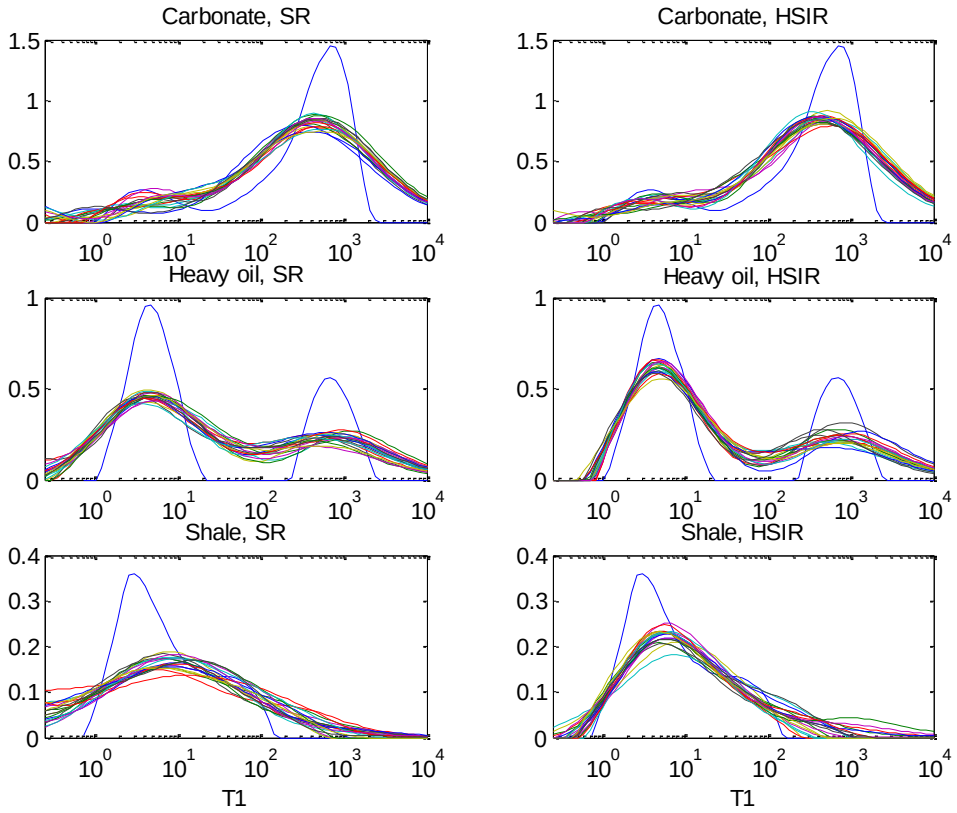

Fig. 4. Comparison between the model (the blue curves) and inversion results from SR (left) and HSIR (right) sequences. The noise level in the model echo train is 0.5 p.u., corresponding to 12–44 SNR, representative to logging data quality. The HSIR results recover the model distribution patterns more closely, and the improvements over SR results are more significant for the poorer-quality data than the high-SNR data shown in Fig. 3.

(c) Optimization of TW

Intuitively, and from Eq. (8), one recognizes that the advantage of using the HSIR sequence over the SR sequence is dependent on the selection of the TW and TI values, as well as the T_1 distribution of the system in investigation. To find the optimal TW parameter, we simulated the heavy-oil and shale gas cases with different TW time and subsequently computed their corresponding Fréchet distance and the curve misfit. In all cases, the SNR is kept at 20. The results are shown in Figs. 5 and 6 for heavy-oil and shale gas cases, respectively.

For both cases, we see that the minimum Fréchet distance and misfit consistently reside at approximately 10 ms. The fact that the optimal TW does not vary significantly from one formation scenario to another is helpful in implementing the HSIR sequence in the logging data-acquisition scheme. As we know, pore sizes and fluid saturations inevitably vary from depth to depth, and the variations are not predictable before logging operations; thus, it is desirable to use one set of parameters to log an entire well.

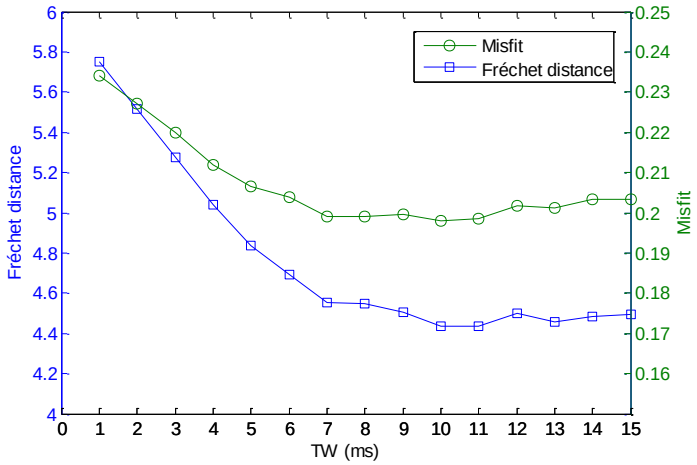

Fig. 5. Searching for the optimal TW in the HSIR sequence. For the representative heavy oil formation case, the optimal TW is approximately 10 ms, based on both the Fréchet distance and curve misfit calculations.

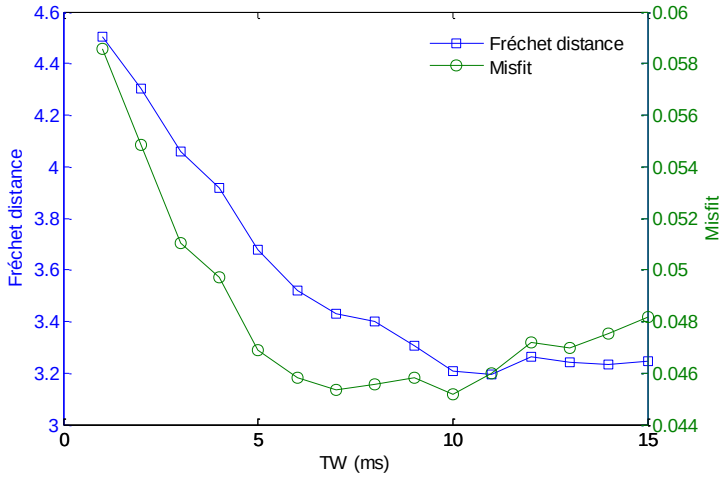

Fig. 6. Searching for the optimal TW in the HSIR sequence for the representative gas shale formation case. The optimal TW is at also approximately 10 ms, based on both the Fréchet distance and curve misfit calculations.

CONCLUSIONS

A hybrid saturation-inversion-recovery (HSIR) sequence is proposed and described for T_1 measurement. Extensive simulations are conducted on representative carbonate formations containing microporosity, heavy oil-bearing formations with movable water, and gas shale formations for the demonstration of the advantages of using the new HSIR sequence over the routinely-used saturation-recovery (SR) sequence in NMR well-logging operations. To compare the resemblance of the model T_1 distribution with the inversion results derived from either HSIR or SR data, Fréchet distance is used as the quantitative measurement. We found that for all cases and for noise levels corresponding

to typical core NMR measurements and logging data, the Fréchet distance is consistently shorter for results derived from the HSIR sequence over that from the SR sequence. Furthermore, we derived the optimal TW in HSIR sequence based on the minimal Fréchet distance and curve misfit.

ACKNOWLEDGEMENTS

The authors would like to thank Halliburton for permission to publish this paper.

REFERENCES

1. Akkurt, R. 2010. System and methods for T1-based logging. US Patent No. 7755354.
2. Meiboom, S. and Gill, D. 1958. Modified spin-echo method for measuring nuclear relaxation times. *Rev Sci Instrum* **29**(8): 688–691.
3. Fukushima, E. and Poeder, S.B.W. 1981. Experimental Pulse NMR, A Nuts and Bolts Approach. Addison-Wesley Publishing Co.
4. Fréchet, M.R. 1941. Sur la loi de répartition de certaines grandeurs géographiques. *Journal de la Société de Statistiques de Paris* **82** 114–122.
5. Eiter, T. and Mannila, H. 1994. Computing discrete Frechet distance. Technical Report 94/64. Christian Doppler Laboratory, University of Vienna.